TOWARDS SUBGRID SCALE MODELING OF SUPPRESSANT FLOW IN ENGINE NACELLE CLUTTER*

P. E. DesJardin, J. M. Nelsen, L. A. Gritzo
A. R. Lopez, and J. M. Suo-Anttila
Sandia National Laboratories

D. R. Keyser and T. A. Ghee
NAVAIR

P. J. Disimile
Wright-Patterson Air Force Base

J. R. Tucker
Applied Research Associates

INTRODUCTION

The release and transport of a suppressant agent into an enclosed compartment is sensitive to local geometrical features or "clutter" that is difficult to resolve numerically without using an excessively large CFD grid. Such examples include wire bundles or hydraulic lines in engine compartments of either ground vehicles or aircraft. Capturing these features on a grid will result in extremely small time steps for explicit time-accurate numerical simulations of agent release and subsequent fire suppression. An alternative approach is to use a subgrid scale (SGS) model to represent the macroscopic effects of these small features using reasonably sized CFD grid cells.

The focus of this research is to develop engineering models of flow, fire, and fire suppression and extinguishment in cluttered environments. These models will advance the fundamental knowledge of fire dynamics and suppression and provide a foundation for optimizing the distribution of suppressants for newly designed or retrofit fire safety systems in aircraft engine nacelles. This work is being carried out in a joint, iterative computational/experimental approach to develop engineering subgrid models for use in integral CFD and fire field simulations. These subgrid models will be used to represent phenomena too small to resolve using a computational mesh (with smaller length scales on the order of 10 cm). Models will he developed using detailed CFD calculations performed at SNL and discovery and validation experiments performed at Air Force and Naval laboratories. Only gaseous agents will he investigated initially. The end goal is to provide computational tools to improve suppressant delivery by reducing the need to model the fine geometries in the cluttered regions of the engine in the nacelle.

For agent dispersal in a cold flow environment the effects of subgrid clutter have two main effects on the macroscopic flow field. The first is to provide a momentum sink due to viscous and pressure drag forces due to the gas flowing through clutter. The second is to either increase or decrease the turbulent kinetic energy levels depending on the local clutter size, l_C, relative to the characteristic length scale of turbulence, l_T. In general, if $l_C < l_T$ the turbulent kinetic energy will decrease and if $l_C > l_T$ the turbulent kinetic energy will increase. For flame suppression the clutter also serves as either a mechanism for flame attachment or local extinction depending on the local time scales of the heat transfer to the clutter and chemical kinetics for ignition, although these issues will not be the focus of this paper.

A literature search reveals little available information in the area of subgrid modeling of cluttered spaces. The closest to cluttered environments is numerical modeling of rigid porous structures for high Reynolds number flow. Readers interested in the state-of-the-art in this area can consult these papers [1–6], which provide details of the available means to define the time and phase averaged transport equations for momentum transport as well as derivations of the turbulent kinetic energy transport appropriate for porous flows. This effort is to extend these approaches to clutter environments for which the length scale of the clutter is not small relative to the size of the system.

* This work was performed in part at Sandia National Laboratories, a multiprogram laboratory operated by Sandia Corporation, a Lockheed-Martin Company, for the US Department of Energy, contract DE-AC04-94AL85000.

The rest of the paper starts with the mathematical formulation of the clutter model based on spatial filtering concepts. The filtering of the governing equations result in unknown correlations that require modeling. Constitutive models are formulated based on a linear combination of porous media and bluff body lift and drag relations along with results showing predictions using these models for a density and loosely packed clutter. Results are then presented of macroscopic predictions of turbulent flow in the limit of porous media with comparisons to detailed CFD calculations available from the literature. Next, experimental measurements of a cylinder in a turbulent cross flow are presented along with detailed CFD predictions. Finally conclusions are drawn and future efforts summarized.

MATHEMATICAL MODEL FORMULATION

The following mathematical description is limited to a summary of the development of stationary clutter. The section *starts* with an introduction to the two-phase (i.e., spatial) averaging and time averaging. The reasons for reviewing these mathematical formalities are to familiarize the reader with the concepts of spatial filtering and, more importantly, highlight the restrictions imposed by this approach with respect to the implementation of the clutter model into a CFD code. Next, these averaging concepts are applied to the conservation equations of momentum turbulent kinetic energy transport resulting in unknown second order correlations and surface integral terms, which represent subgrid physics that must be closed with a clutter model. Requirements for the clutter model are provided based on both physical and computational requirements. The end result of this section is to provide a closed set of phase and time averaged transport equations for momentum, turbulent kinetic energy, and turbulent kinetic energy dissipation rate.

TWO-PHASE AVERAGING

The formal averaging for two-phase media was first introduced by Anderson and Jackson [7] through the use of a local filtering function and later refined by Gray and Lee [8] and Gough and Zwarts **[9]** as presented in textbook form by **Kuo** [10]. Alternatively, Slattery [11] offers a different derivation based on a spatially dependent volume of integration. The presentation here follows the outline of Kuo. Figure 1 illustrates a typical phase averaging volume showing the total volume of interest, V_T, the volume of the solid clutter, V_C, and the volume of the gas, V_g.

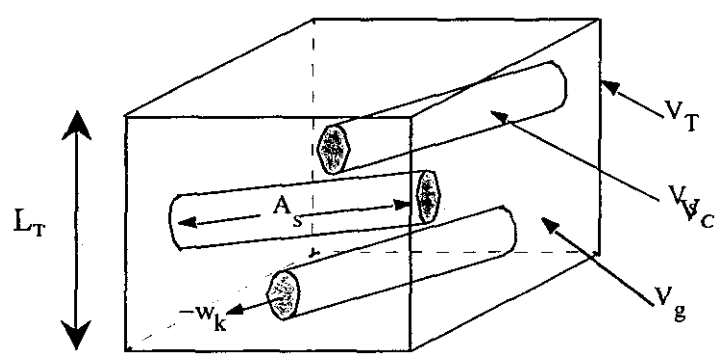

Figure 1. Phase averaging volume.

Phase averaged properties are obtained by first defining a spatial filtering function, $G\left[(x_i - x_i')/\Delta_f\right]$, with the normalization property: $\int_{V_\infty} G\left[(x_i - x_i')/\Delta_f\right] dV' = 1$. For volume averaging using a cubic volume of length $L_T = (V_T)^{1/3}$ on a side then $\Delta_f = L_T$ and G is defined as

$G = \frac{1}{V_T}\prod_{i=1}^{3}\left[H\left(x_i' - x_i + \Delta_i/2\right) - H\left(x_i' - x_i - \Delta_i/2\right)\right]$ where H is the Heaviside function. Convoluting G with the a gas property of interest, β, yields a **gas** phase average quantity,

$$\hat{\beta}(x_i) = \int_{V_{g_\infty}} \beta(x_i')G\left(\frac{x_i - x_i'}{\Delta_f}\right) dV' \tag{1}$$

which physically represents a spatially averaged property over the volume, V_T. It should be emphasized that the volume of integration, V_{g_∞}, represents **all** of regions occupied by the gas and so does not depend on the location, x_i, where the averaging takes place. Of more value is the intrinsic average, $\langle\beta\rangle$, defined as the local average of β over the gas phase volume, V_g, for which constitutive and thermodynamic properties are well defined. The intrinsic average is defined as: $\langle\beta\rangle = \hat{\beta}/\phi$ and is the variable of interest to solve for after phase averaging the transport equations for mass, momentum and energy. The variable, ϕ, is the void fraction and is defined as the volume of gas divided by the averaging volume, i.e., $\phi \equiv V_g / V_T$.

TEMPORAL AND SPATIAL DERIVATIVES FOR PHASE AVERAGING

Applying the spatial filtering function to the transport equations requires expressing the phase averaged time and spatial partial derivatives in terms of temporal and spatial derivatives of phase averaged quantities. In the following development, the volume of the gas phase is assumed to change as a function of both time and space to accommodate the complexities that may be included in future efforts (e.g., decomposing or burning clutter). Simplifications are then imposed to limit the scope to the focus of this work on turbulence modeling on rigid, non-burning clutter.

Time Derivatives

Relations for the temporal derivative are obtained by taking the partial derivative of ϕ.

$$\frac{\partial\hat{\beta}}{\partial t} = \frac{\partial}{\partial t}\int_{V_g(t)} \beta(x_i')G\left(\frac{x_i - x_i'}{\Delta_f}\right) dV' \tag{2}$$

Since the volume of the gas is assumed to be a function of time, Leibnitz rule [12] **has** to be applied to commute the temporal derivative term inside the volume averaging operator **as** follows:

$$\frac{\partial\hat{\beta}}{\partial t} = \int_{V_{g_\infty}(t)} G\left(\frac{x_i - x_i'}{\Delta_f}\right)\frac{\partial\beta(x_i')}{\partial t} dV' + \int_{A_{g_\infty}(t)} G\left(\frac{x_i - x_i'}{\Delta_f}\right)\beta(x_i')w_k(x_i') dA_k' \tag{3}$$

In **Eq.** (3), the first term on the right hand size is simply the definition of the phase averaged time rate in change of β, i.e., $\widehat{\partial\beta/\partial t}$. The second term is a surface integral that accounts for material crossing the boundary of the phase averaging volume as a function of time where w_k is the velocity of the surface (pointing into the solid clutter [Figure 1]) of the **gas** phase volume, V_g, on the surface, A, . The gas phase surface can be further broken into the contribution associated with the clutter, A_c, **and** rest of the surface area associated with the phase averaging volume, A_{g-c}. Since G goes to zero at the boundary on the surface A_{g-c} then that contribution of the surface integral is equal to zero leading to the following relation for the phase averaged time derivative that will become useful when deriving the phase averaged transport equations.

$$\widehat{\frac{\partial \beta}{\partial t}} = \frac{\partial}{\partial t}\hat{\beta} - \int_{A_{g\infty}(t)} G\left(\frac{x_i - x_i'}{\Delta_f}\right)\beta(x_i')w_k(x_i')\,dA_k' \tag{4}$$

In addition, the clutter surface is assumed rigid and non-porous so that the normal velocity to the clutter surface is identically zero (i.e., $w_k = 0$) allowing for the temporal derivative to commute with the filter operation resulting in the simple relation.

$$\widehat{\frac{\partial \beta}{\partial t}} = \frac{\partial}{\partial t}\hat{\beta} \tag{5}$$

Space Derivatives with Uniform Filter Width (i.e., $\Delta_f = const$)

Analogous to the time derivatives, a spatial derivative relation is obtained by taking the divergence of a phase averaged vector quantity.

$$\frac{\partial}{\partial x_j}\hat{\beta}_j(x_i) = \frac{\partial}{\partial x_j}\int_{V_{g\infty}} \beta_j(x_i')G\left(\frac{x_i - x_i'}{\Delta_f}\right)dV' \tag{6}$$

Since the volume averaging is independent of the location the partial derivative can be brought inside the integration and applied directly to the filtering function G.

$$\frac{\partial}{\partial x_j}\hat{\beta}_j(x_i) = \int_{V_{g\infty}} \beta_j(x_i')\frac{\partial}{\partial x_j}G\left(\frac{x_i - x_i'}{\Delta_f}\right)dV' \tag{7}$$

For uniform filter size (i.e., A, $= const$) then $\partial G/\partial x_j = -\partial G/\partial x_j'$ and using the chain rule of differentiation then Eq. (7) can be expressed as:

$$\frac{\partial}{\partial x_j}\hat{\beta}_j(x_i) = \int_{V_{g\infty}} \left\{G\left(\frac{x_i - x_i'}{\Delta_f}\right)\frac{\partial \beta_j(x_i')}{\partial x_j'} - \frac{\partial}{\partial x_j'}\left[\beta_j(x_i')G\left(\frac{x_i - x_i'}{\Delta_f}\right)\right]\right\}dV' \tag{8}$$

The first term on the right side of Eq. *(8)* is the two-phase average of the gradient of the vector quantity; the second term can be further expressed in terms of a surface integral using the divergence theorem. Re-arranging terms leads to an expression for the phase averaged divergence of a vector quantity in terms of the divergence of a phase averaged quantity and a surface integral to account for microscopic clutter effects.

$$\widehat{\frac{\partial \phi_j(x_i)}{\partial x_j}} = \frac{\partial \hat{\phi}_j(x_i)}{\partial x_j} + \int_{A_c} \phi_j(x_i')dA_j' \tag{9}$$

An important assumption in the derivation of Eq. (9) is ***the filter width is assumed to be constant;*** i.e., the filter width is assumed to be invariant with space and time. Alternatively, the development of a nonuniform filter width could be pursued for which $\partial G/\partial x_j \neq -\partial G/\partial x_j'$. However, the introduction of such a filter brings in commutation error that has been discussed in the Large Eddy Simulation (LES) literature [13, 14, 15] as well a surface integral error term. The former of these two sources of error has been somewhat mitigated using filter functions that satisfy commutivity up to some order of accuracy [15]. However, the second source of error is more difficult to treat and leads to a violation of mass, momentum, and energy conservation when these quantities are exchanged among phases [16]. These issues are not merely academic. Often in practice the filter width is assumed to be proportional to the local grid size, e.g., $\Delta_f = C\Delta_x$, where Δ_x is the local grid cell size and C is a constant that is greater or equal to one. Therefore, in a practical engineering problem where the CFD grid cell size changes in space, then

the assumption of $\mathbf{A}_c = const$ is violated! In order to avoid this contradiction, ***the filter width is assumed to be independent from the grid.*** This choice also has the added benefit to allowing for grid convergence (see requirement 4, discussion below). The disadvantages of a filter width independent of the grid are two fold, First, the clutter model must be able to capture the relevant physics over a wide range of filter to clutter size ratios (see requirement 1 of discussion below). Second, the coding of the clutter model is further complicated with the introduction of an integral of the clutter source terms to account for the effects of intermittency (see requirement 3, discussion below).

Only phase averaging concepts have been briefly reviewed. In addition, it is also desirable to time average the governing equations of mass, momentum and energy transport to remove any remaining high frequency turbulence signal and to be compatible with the Reynolds Averaged Navier Stokes (RANS) transport equations that are commonly used for solving practical engineering applications. Time averaging issues are not reviewed in this paper since excellent discussions of time averaging concepts are provided in several introductory texts on turbulence [17].*

PHASE AND TIME AVERAGING OF TRANSPORT EQUATIONS

Applying the phase averaging relations given by **Eqs.** *(5)* and **(9)** in addition to time averaging to the transport equations of momentum, turbulent kinetic energy and turbulent dissipation leads to the following set of transport equations.

Momentum

$$\rho\left[\frac{\partial}{\partial t}\left(\phi\langle\bar{u}_j\rangle\right)+\frac{\partial}{\partial x_i}\left(\phi\langle\bar{u}_i\rangle\langle\bar{u}_j\rangle\right)\right]=-\frac{\partial\left(\phi\langle\bar{p}\rangle\right)}{\partial x_i}+\frac{\partial\phi\langle\overline{\tau_{ij}}\rangle}{\partial x_i}-\int_{A_c}\left[\bar{p}\delta_{ij}-\overline{\tau_{ij}}\right]n_i dA'-\frac{\partial\phi\left\langle\overline{u_i'u_j'}\right\rangle}{\partial x_i} \tag{10}$$

Turbulent Kinetic Energy

$$\begin{aligned}&\rho\left[\frac{\partial}{\partial t}\left(\phi\langle k\rangle\right)+\frac{\partial}{\partial x_i}\left(\phi\langle\bar{u}_i\rangle\langle k\rangle\right)\right]=\mu\frac{\partial^2}{\partial x_i\partial x_i}\left(\phi\langle k\rangle\right)-\rho\phi\langle\varepsilon\rangle\\&-\rho\left\{\phi\left\langle\overline{u_i'u_j'}\right\rangle\frac{\partial\langle\bar{u}_i\rangle}{\partial x_j}+\frac{\partial}{\partial x_i}\left[\phi\left\langle u_i'\left(p'/\rho+u_k'u_k'/2\right)\right\rangle\right]\right\}-\rho\left\{\phi\left\langle\left(\overline{u_i'u_j'}\right)\left(\frac{\partial\overline{u_i}}{\partial x_j}\right)\right\rangle+\frac{\partial}{\partial x_i}\left(\phi\left\langle\left(\overline{u_i}\right)k\right\rangle\right)\right\}\end{aligned} \tag{11}$$

Turbulent Kinetic Energy Dissipation (i.e., $\varepsilon\equiv\overline{\mu\left(\partial u_i'/\partial x_i\right)\left(\partial u_j'/\partial x_i\right)}/\rho$)

$$\begin{aligned}&\rho\left[\frac{\partial}{\partial t}\left(\phi\langle\varepsilon\rangle\right)+\frac{\partial}{\partial x_i}\left(\phi\langle\bar{u}_i\rangle\langle\varepsilon\rangle\right)\right]=-\phi\left\langle 2\mu\frac{\partial\bar{u}_j}{\partial x_k}\left\{\overline{\frac{\partial u_j'}{\partial x_l}\frac{\partial u_k'}{\partial x_l}}+\overline{\frac{\partial u_i'}{\partial x_j}\frac{\partial u_i'}{\partial x_k}}\right\}\right\rangle\\&-\phi\left\langle 2\mu\left\{\overline{\frac{\partial u_j'}{\partial x_k}\frac{\partial u_j'}{\partial x_l}\frac{\partial u_k'}{\partial x_l}}+\frac{\mu}{\rho}\overline{\left(\frac{\partial^2u_j'}{\partial x_k\partial x_l}\right)^2}\right\}\right\rangle-\phi\left\langle\mu\frac{\partial}{\partial x_k}\left\{\overline{u_k'\frac{\partial u_j'}{\partial x_l}\frac{\partial u_j'}{\partial x_l}}+\frac{2}{\rho}\overline{\left(\frac{\partial u_k'}{\partial x_l}\frac{\partial p'}{\partial x_l}\right)}\right\}\right\rangle\\&-\phi\left\langle 2\mu\frac{\partial^2u_j}{\partial x_l\partial x_k}\left\{\overline{u_k'\frac{\partial u_j'}{\partial x_l}}\right\}\right\rangle+\phi\left\langle\mu\frac{\partial^2\varepsilon}{\partial x_l\partial x_l}\right\rangle-\rho\frac{\partial}{\partial x_k}\left\{\phi\left\langle u_k'\varepsilon\right\rangle\right\}\end{aligned} \tag{12}$$

wt re the $\langle\overline{...}\rangle$ notation refers to a time and phase averaged quantity. The terms involving $(...)'$ 1 $'(...)$ represent higher order correlation terms of fluctuating quantities in time and space, respectively, which in

* DesJardin, P.E., and Gritzo, **L.A.,** ***On the Development of a Clutter Model for Turbulent Flows,*** 2001. Copy on **file** with the author.

general are unknown and require modeling. The surface integral term in Eq. (10) represents momentum exchange between the surface of the clutter and the surrounding gas due to viscous and pressure drag forces, and the term requires modeling. Note, the surface integral terms only arise in the momentum transport due to assumption that the clutter is rigid (i.e., no melting or burning of clutter). Also, in the derivation the density is assumed to be constant, and second order correlations associated with mass and momentum diffusion have also been neglected.

In Eq. (10), the term $\left\langle \overline{u_i'' u_j''} \right\rangle$ represents the effects of the subgrid fluctuations in time and space and is defined as: $\left\langle \overline{u_i'' u_j''} \right\rangle = \left\langle \overline{u}_i \right\rangle \left\langle \overline{u}_j \right\rangle - \left\langle \overline{u_i u_j} \right\rangle$. This term, the correlations of Eqs. (11) and (12), and the surface integrals of Eq. (10) are closed using models that satisfy a set of guiding principles based on the requirements for modeling the clutter in engine nacelles. These requirements are illustrated below.

1. The constitutive model(s) should be able to accommodate a spectrum of clutter sizes, ranging from a single object (i.e., drag) to many objects that are randomly placed (i.e., clutter that resembles porous media) since the filter width of the phase averaging is assumed to be constant.

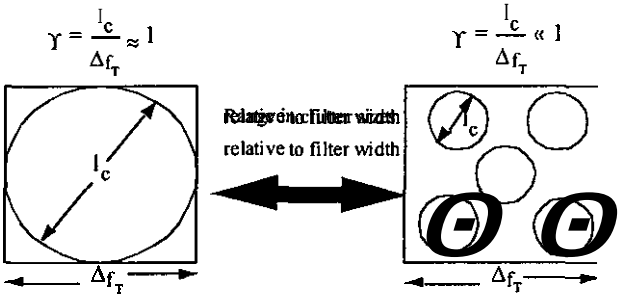

2. The constitutive model(s) should provide a mechanism to represent isotropic (i.e., rotationally invariant) as well as anisotropic (rotationally dependent) clutter with minimal amount of user input.

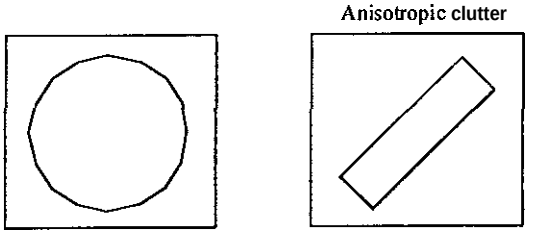

3. The constitutive model(s) should allow for intermittency within the filtering volume so that non-periodic SGS clutter may be addressed.

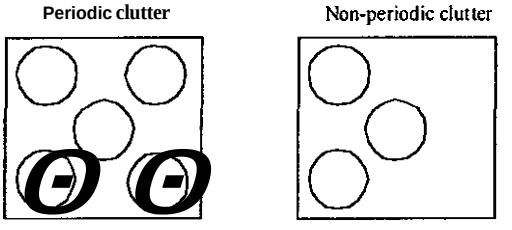

4. **The constitutive model(s) should allow for grid convergence studies to be performed. This implies that the numerical grid should be chosen independent of the phase averaging filtering volume.**

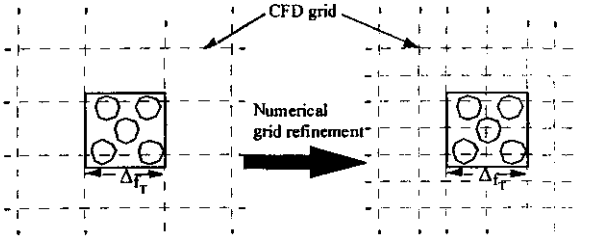

Applying the above guidelines, the final form for the closure terms needed for the phase and time averaged momentum transport equations is as follows:

$$-\frac{\partial\phi\left\langle \overline{u_i'\,u_j'}\right\rangle}{\partial x_i}-\int_{A_c}\left[\overline{p}\delta_{ij}-\overline{\tau_{ij}}\right]n_j dA'=\frac{\partial}{\partial x_i}\left[\phi(\mu_T+(1-\psi)\mu_B)\left(\frac{\partial\langle\overline{u}_j\rangle}{\partial x_i}+\frac{\partial\langle\overline{u}_i\rangle}{\partial x_j}\right)\right]$$

$$-\frac{1}{\Delta^3_f}\int_{V_T}\left[\underbrace{(1-\psi)\phi^2\left(\langle\overline{\mu}\rangle\frac{\langle\overline{u}_p\rangle}{K}+\frac{\rho\phi C_{CM_2}}{\sqrt{K}}\left|\langle\overline{u}_k\rangle\right|\langle\overline{u}_j\rangle\right)}_{\mathbf{S_P}}-\underbrace{\psi\frac{\rho A_p C_D}{2\Delta^3_f}\left|\langle\overline{u}_k\rangle\right|\langle\overline{u}_j\rangle}_{\mathbf{S_B}}\right]GdV \qquad (13)$$

$\mathbf{S_P}$ = Porous media term (i.e., modified Darcy-Forchheimer Law)

$\mathbf{S_B}$ = Bluff body drag/lift term

The first term on the right side of Eq. (13) represents the effects of microscopic dispersion and turbulent fluctuations using Brinkman [1 **8,191,** μ_B, and turbulent eddy [20], μ_T, viscosity models, respectively. On the second line of Eq. (13), ψ $(=l_C/\Delta_f)$ is a the ratio the length scale of the clutter to the size of the filtering volume and serves as a linear weighting function to blend constitutive models from the porous media literature [21,22,23] with simple bluff body lift and drag models [24,25]. **A** linear blending is not unique and other weightings could be chosen. An assessment of using a linear blending of constitutive models from the porous media and bluff body drag is investigated for a collection of spheres. Figure 2 (a) and (b) show results ofthe drag force per unit volume using a modified Darcy-Forchheimer Law (i.e., $F_j/\Delta_f{}^3=\phi^2\langle\overline{u}_j\rangle\left[\langle\overline{\mu}\rangle/K+C_{M2}\phi\left|\langle\overline{u}_k\rangle\right|/\sqrt{K}\right]$) for and a bluff body drag for a linear superposition of a collection of spheres (i.e., $F_j/\Delta_f{}^3=(2/3)N\rho\left|\langle\overline{u}_k\rangle\right|\langle\overline{u}_j\rangle(1-\phi)C_D/D$). In the Darcy-Forchheimer relation, $K\left(\equiv-\mu\phi\langle u_j\rangle/(\partial p/\partial x_j)\right)$is the permeability and is determined using the empirical relation $K=\phi^3D^2/\left[C_{M1}(1-\phi)^2\right]$ where C_{M1} is set equal to 147 [5] and C_{M2} is set to two values of either 1.75 corresponding to the values suggested by Kuwahara et al. [5] for spheres or 2.3 from the classical result of Ergun [26] which is considered independent of local geometry. The results show that the porous media and bluff body drag have a similar functional dependence on the Reynolds number with the two predicting almost the same force per unit volume for either low porosity at high Reynolds number or for high porosity at low Reynolds number. This suggests that the linear blending of these two limits is a reasonable approach to span the possible range of clutter sizes.

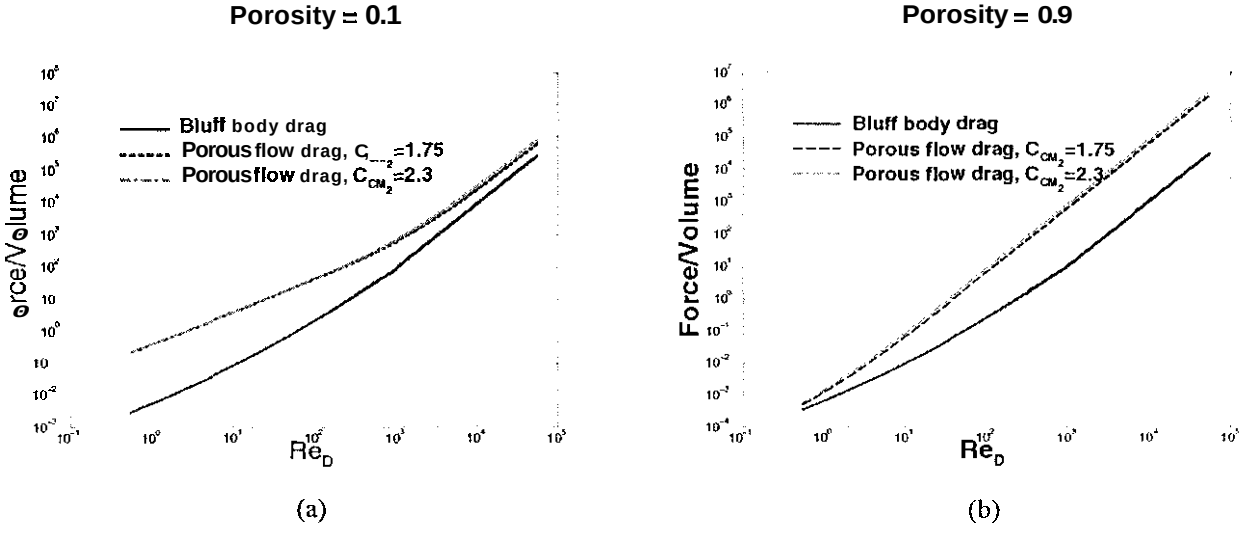

Figure 2. Force/volume using constitutive models for a collection of spheres from porous media and bluff body drag relations using a porosity of (a) 0.1 and (b) 0.9.

Due to space constraints, the details of the closure k and ε equations will be omitted. Instead, a summary of the modeled form of the right side (RHS) of **Eqs.** (11) and (12) is provided below. Details of these closure terms can be found in Refs. [1] and [17].

$$\text{RHS of Eq. (11)} = \frac{\partial}{\partial x_i}\left[(\mu+\mu_T)\frac{\partial}{\partial x_i}\left(\phi\langle k\rangle\right)\right] - \rho\phi\left\langle\overline{u_i'u_j'}\right\rangle\frac{\partial\left(\phi\langle\bar{u}_j\rangle\right)}{\partial x_i} + \frac{1}{\Delta_f^{\,3}}\int_{V_T}\langle k\rangle\left(S_P+S_B\right)/\left(\phi\langle\bar{u}_j\rangle\right)GdV - \rho\phi\langle\varepsilon\rangle \quad (14)$$

$$\text{RHS of Eq. (12)} = \frac{\partial}{\partial x_i}\left[(\mu+\mu_T)\frac{\partial}{\partial x_i}\left(\phi\langle\varepsilon\rangle\right)\right] - C_{\varepsilon 1}\rho\left\langle\overline{u_i'u_j'}\right\rangle\frac{\partial\left(\phi\langle\bar{u}_j\rangle\right)}{\partial x_i}\frac{\langle\varepsilon\rangle}{\langle k\rangle} + \frac{1}{\Delta_f^{\,3}}\int_{V_T}C_{\varepsilon 2}\rho\langle\varepsilon\rangle\left\{C_k S_P + S_B\right\}G/\left(\phi\langle\bar{u}_j\rangle\right)dV \quad (15)$$

NUMERICAL IMPLEMENTATION

The clutter models discussed in the previous section are implemented in a general-purpose fire simulation code, VULCAN, which is based **on** the KAMELEON-Fire code [27]. VULCAN uses a RANS-based model suite including a k-ε turbulence model [28]. Numerical discretization is **on** a staggered, block-structured grid with second-order upwind differencing **for** the convective terms using a version of the SIMPLE algorithm [29]. Previous studies using VULCAN for pool fire simulations can be found in references [30, 31,321. The source terms appearing in Eq. **(13)** for momentum transport are treated in a semi-implicit nature to maintain numerical stability. **The** source terms appearing in **Eqs.** (14) and **(15)** are implemented in an explicit manner.

RESULTS

Two limiting cases are under consideration for assessing the clutter model. The first is unidirectional flow in periodic porous media (Figure 3). Figure 4 (a) and (b) show predictions of normalized turbulent kinetic energy and its dissipation rate as a function of downstream locations using the macroscopic clutter model. The initial kinetic energy and dissipation rate are chosen to be 10 and **30** times the steady-state

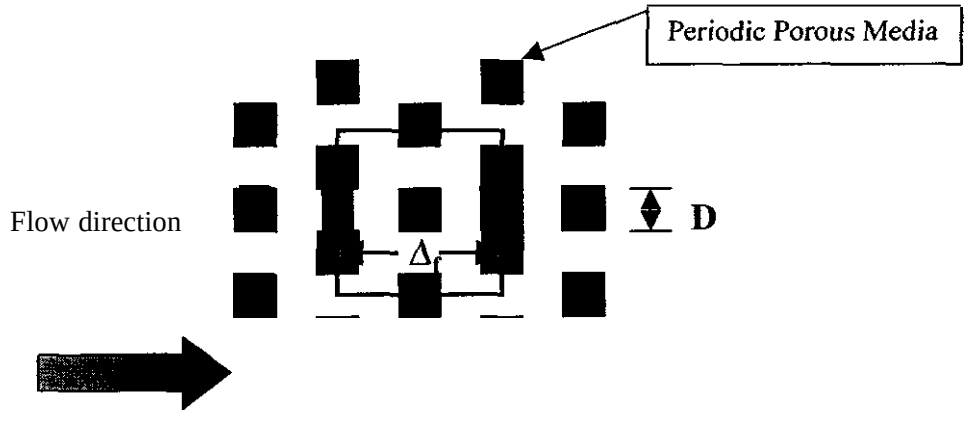

Figure **3:** Schematic of periodic porous media problem

values, respectively, in order **to** match the previous studies of the same problem [1, 4]. Predictions using the clutter model agree well with these previous studies in this limiting where the clutter model degenerates to just the porous media contribution.

The second problem under consideration is a cylinder in well-characterized homogeneous turbulent flow. The cylinder shape was chosen since this shape is representative of the class of clutter objects typically encountered in aircraft engine nacelles. Experimental measurements are taken at the US Naval Academy (USNA) using their low-speed (0 to 20 m/s) tunnel (Figure 5), for which high turbulence (–10%) could be obtained. Hot wire anemometry is used to measure instantaneous stream-wise velocity to obtain mean

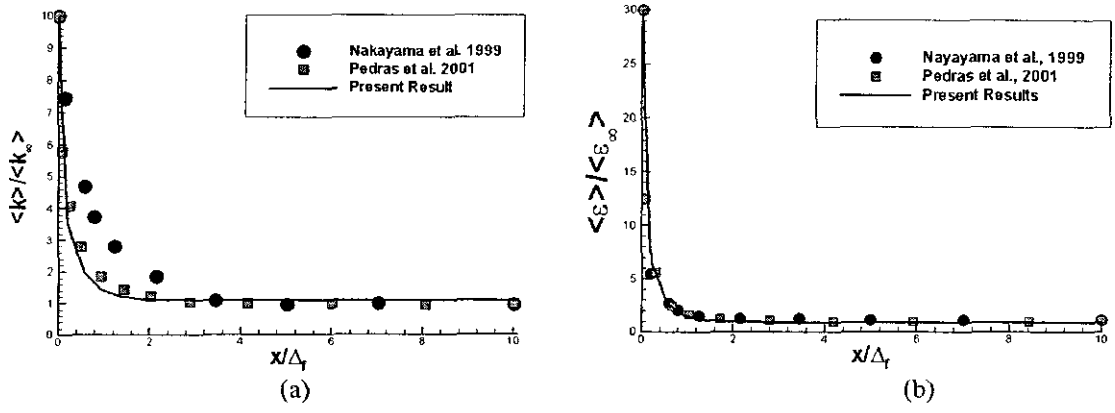

Figure **4.** Normalized turbulent kinetic energy and its dissipation rate verses x/Δ_f using clutter model in the limit of porous media.

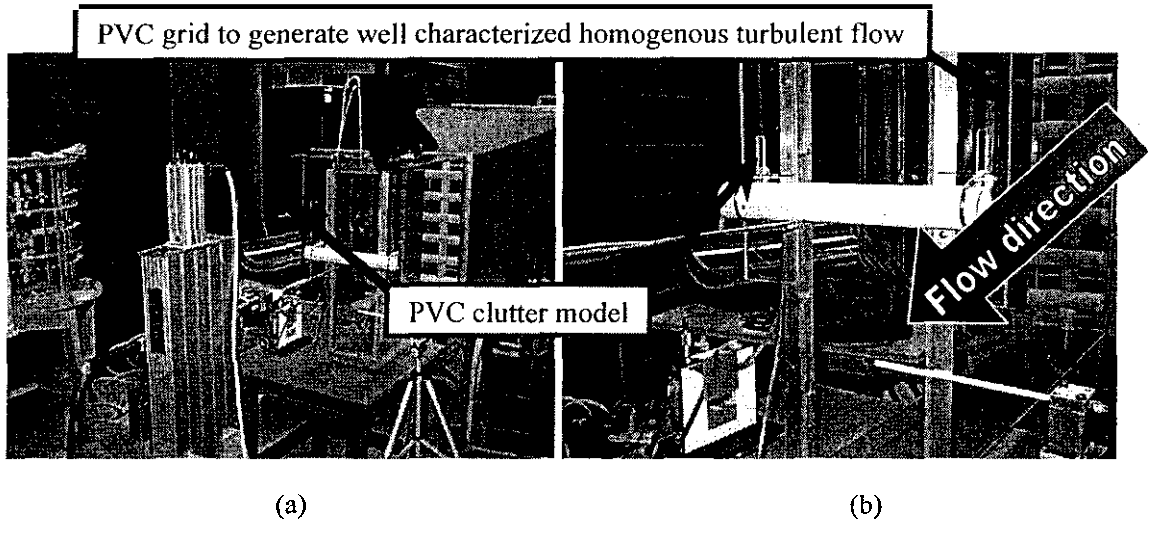

Figure 5. (a) USNA wind tunnel facility and (b) blow up region ofcylinder representing clutter object under highly turbulent flow conditions.

and RMS profiles before and after the cylinder. Figures ***6*** and 7 include measurements (shown with symbols) of mean and **RMS** stream-wise velocity, respectively. Based on a momentum balance calculation, the coefficient of drag (C_D) is determined to be **0.97,** which is ***24% lower*** than the coefficient of drag of **1.28** calculated without the turbulence generator in place. This result indicates that the effects of upstream turbulence on the drag characteristics of clutter (i.e., the C_D in **Eq.** (13)) are significant.

In Figures ***6*** and 7, 2D CFD predictions using the CFD-ACE software package [33] (shown with lines) are detailed. The purpose of conducting the detailed CFD calculations is to provide full flow field details to construct phase-averaged quantities that cannot be obtained experimentally. These details are needed for calibration of the unknown clutter model coefficients in the bluff body drag limit. As shown in these figures, good qualitative agreement to the experimental data is observed for the mean and RMS. Quantitatively, the numerical predictions do appear to underpredict the extent of the velocity deficit profile as well as the wake region ofthe cylinder. These differences may be attributed to the limitations performing a 2D calculation (i.e., **no** streamwise vorticity generation captured **for** enhanced mixing) and the use of the k-ε turbulence model in strongly recirculating flows (i.e., k-ε model assumes local isotropy). Both of these issues are currently being explored by performing 3D calculations using more

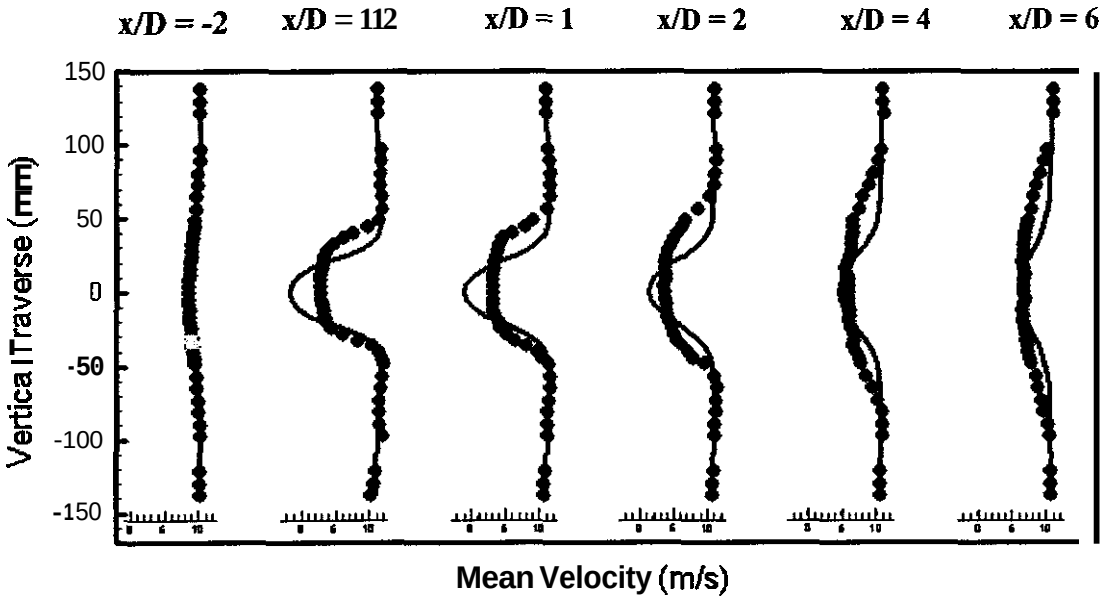

Figure **6.** Comparisons of mean streamwise velocity profiles at several down stream locations. Solid lines are CFD predictions and symbols are experimental measurements.

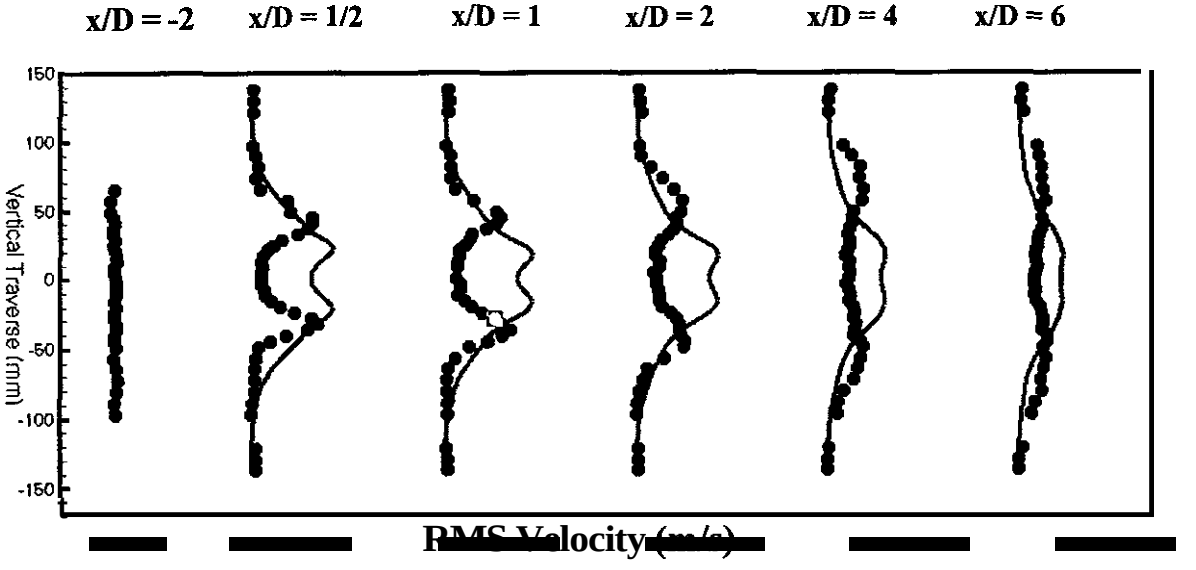

Figure 7. Comparisons of RMS streamwise velocity profiles at several down stream locations. Solid lines are CFD predictions and symbols are experimental measurements.

advanced turbulence models. The reasonable agreement of the CFD predictions to the experimental data in Figures 6 and 7 supports the use of detailed CFD for clutter model calibration.

CONCLUSIONS

A preliminary clutter model has been formulated based on the use of two-phase averaging concepts. The implementation of phase averaging introduces constraints onto the requirements of the clutter model. The most stringent of these constraints is that the model must be able to represent a wide range of clutter length scales ranging from a porous media limit to bluff body drag. This requirement is satisfied using a

linear combination of constitutive models from the porous media literature and relations for bluff body drag. Based on this formulation, two simplified problems are considered for calibration of the model constants: (1) the first is turbulent flow in a porous media for which a preliminary version of the clutter model is able to reproduce established trends taken from the literature; (2) the second is subjecting a cylinder to a highly turbulent cross flow for which there are little existing published data. Results of experimental measurements show a significant decrease in drag coefficient due to the highly turbulent inflow. Detailed numerical predictions of the same problem show good qualitative agreement to experimental measurements indicating that the use of detailed spatial information from CFD results is a valid approach for clutter model calibration. Future work is to perform this calibration so that the macroscopic model will be able to reproduce the trends in the bluff body limit. In addition, the model will be extended beyond the unidirectional treatment presented here to anisotropic cluttered environments.

ACKNOWLEDGMENTS

This work is supported by the US Department of Defense Program under the Next-Generation Fire Suppression Program.

REFERENCES

1. Pedras, M.H.J., and de Lemos, M.J.S., "Macroscopic Turbulence Modeling for Incompressible Flow Through Undeformable Porous Media," *International Journal of Heat and Muss Transfer,* 44, pp. 1081-1093,2001.
2. Pedras, M.H.J., and de Lemos, M.J.S., "Simulation of Turbulent Flow in Porous Media Using a Spatially Periodic Array and a Low Re Two-Equation Closure,'' *Numerical Heat* Transfer, 39, pp. 35-39, 2001.
3. Pedras, M.H.J., and de Lemos, M.J.S., "On the Definition of Turbulent Kinetic Energy for Flow in Porous Media," *Comm. Heat Mass Transfer*, 21, pp. 211-220, 2000.
4. Nakayama, A., and Kuwahara, F., "A Macroscopic Turbulence Model for Flow in a Porous Medium," *Journal of Fluids Engineering,* 121, pp. 427-433, 1999.
5. Kuwahara, F., Kameyama, Y., Yamashita, S., and Nakayama, A., "Numerical Modeling of Turbulent Flow in Porous Media Using a Spatially Periodic Array," *Journal of Porous Media,* I, pp. 47-55, 1998.
6. Antohe, B.V., and Lage, J.L., "A General Two-Equation Macroscopic Turbulence-Model for Incompressible Flow in Porous Media," *Int. J. Heat Mass Transfer,* 40, pp. 3013-3024, 1997.
7. Anderson, T.B., and Jackson, R., "A Fluid Mechanical Description of Fluidized Beds," *I&EC Fundamentals,* **6,** pp. 527-539, 1967.
8. Gray, W.G., and Lee, P.C.Y., "On the Theorems for Local Volume Averaging of Multiphase Systems," *Int. J. Multiphase* **Flow,** 3, pp. 333-340, 1977.
9. Gough, P.S., and Zwarts, F.J., "Modeling Heterogeneous Two-Phase Reacting Flow," *AIM Journal,* 17, pp. 17-25,]979.
10. Kuo, K.K., *Principles of Combustion*, A Wiley-Interscience Publication, John Wiley & Sons, New York, NY, 1986.
11. Slattery, J.C., *Momentum Energy and Mass Transfer in Continua,* second edition, Robert E. Krieger Publishing Company, Inc., 1981.
12. Kaplan, W., *Advanced Calculus,* Edition 3rd, Addison-Wesley Publishing Company, Reading, MA, pp. 257-259, 1984.
13. Ghosal, S., and Moin, P., "Basic Equations for the Large Eddy Simulation of Turbulent Flow in Complex Geometry," *Journal of Compuational Physics,* I 18, pp. 24-37, 1995.
14. Ghosal, S., "Mathematical and Physical Constraints on Large-Eddy Simulation of Turbulence," *AIM Journal,* 37, pp. 425-433, 1999.

IS. Vailyev, O.V., Lund, T.S., and Moin, P., "A General Class of Commutative Filters for LES in Complex Geometries," Journal ***of Compuational Physics,*** 146, pp. 82-104, 1998.

16. Tennekes, H., and Lumley, J.L., ***A First Course in Turbulence,*** MIT Press, Cambridge, MA, 1972.

17. Pope, S.B., ***Turbulent Flows,*** Cambridge University Press, New York, NY, 2000.

18. Brinkman, H.C., "A Calculation of the Viscous Force Exerted by a Flowing Fluid on a Dense Swarm of Particles," *Appl. Sci.* Res., A1, pp. 27-34, 1947.

19. Brinkman, H.C., "On the Permeability of Media Consisting of Closely Packed Porous Particles," ***Appl. Sci.*** Res., A1, pp. 81-86, 1948.

20. Tennekes, H., and Lumley, J.L., A ***First Course in Turbulence,*** The MIT Press, Cambridge, MA, 1972.

21. Kuwahara, F., Kameyama, Y., Yamashita, S., and Nakayama, A., "Numerical Modeling of Turbulent Flow in Porous Media Using a Spatially Periodic Array," *J.* ***of Porous Meda,*** 1, pp. 47-***55,*** 1998.

22. Whitkar, S., "Advances in the Theory of Porous Media," ***Ind. Engng. Chem.,*** vol. 61, pp. 14-28, 1969.

23. Whitkar, S., "The Transport Equations for Multi-Phase Systems," ***Chemical Engineering Science,*** 28, pp. 139-147, 1973.

24. Blevins, R.D., ***Applied Fluid Dynamics Handbook,*** Van Nostrand Reinhold Company, Inc., New York, NY, pp. 333-334, 1984.

25. Hoerner, S.F., ***Fluid-Dynamic Drag,*** published by author, New York, NY, 1957.

26. Ergun, S., "Fluid Flow Through Packed Columns," ***Chem. Eng., Prog.***, 48, pp. 89-94, 1952.

27. Holen, J., Brostøm, M., and Magnussen, B.F., "Finite Difference Calculation of Pool Fires," In ***Proceedings of 23rd Symp. (Int.)*** on ***Combustion,*** 1677-1683, The Combustion Institute, Pittsburgh, PA, 1990.

28. Jones, W.P., and Launder, B.E., "The Prediction of Laminarization with a Two-Equation Model of Turbulence," ***Int. J. Heat Mass Transfer,*** 15, pp. 301-314, 1972.

29. Patankar, S.V., ***Numerical Heat Transfer and Fluid Flow,*** Hemisphere Publishing Co, New York, NY, 1980.

30. Gritzo, L.A., Nicolette, V.F., Tieszen, S.R., Moya, J.L., and Holen, J., "Heat Transfer to the Fuel Surface in Large Pool Fires," In Chan, S.H., ed., ***Transport Phenomena in Combustion,*** pp. 701-712, Taylor & Francis, 1995.

31 Tieszen, S.R., Nicolette, V.F., Gritzo, L.A., Holen, J., Murray, D., and Moya, J.L., ***Vortical Structures in Pool Fires: Observation, Speculation, and Simulation,*** Technical Report SAND96-2607, Sandia National Laboratories, Albuquerque, NM, 1996.

32. Gritzo, L.A., and Nicolette, V.F., "Coupling of Large Fire Phenomenon with Object Geometry and Object Thermal Response," ***Journal of Fire Sciences,*** 15, pp. 427-442, 1997.

33. ***CFD-ACETM, CFD-ACE Structured Flow Solver Manual,*** Version ***5,*** CFD Research Corporation, Huntsville, AL, October 1998.